Crystal Structures of Human Adenosine Kinase Inhibitor Complexes Reveal Two Distinct Binding Modes†

Steven W. Muchmore,*,‡ Richard A. Smith,‡ Andrew O. Stewart,§ Marlon D. Cowart,§ Arthur Gomtsyan,§ Mark A. Matulenko,§ Haixia Yu,§ Jean M. Severin,‡ Shripad S. Bhagwat,§ Chih-Hung Lee,§ Elizabeth A. Kowaluk,§ Michael F. Jarvis,§ and Clarissa L. Jakob‡

Structural Biology, R46Y, and Neuroscience Research, R4PM, Global Pharmaceutical Research and Development, Abbott Laboratories, 100 Abbott Park Road, Abbott Park, Illinois 60064

Received February 17, 2006

Adenosine kinase (AK) is an enzyme responsible for converting endogenous adenosine (ADO) to adenosine monophosphate (AMP) in an adenosine triphosphate- (ATP-) dependent manner. The structure of AK consists of two domains, the first a large α/β Rossmann-like nucleotide binding domain that forms the ATP binding site, and a smaller mixed α/β domain, which, in combination with the larger domain, forms the ADO binding site and the site of phosphoryl transfer. AK inhibitors have been under investigation as antinociceptive, antiinflammatory, and anticonvulsant as well as antiinfective agents. In this work, we report the structures of AK in complex with two classes of inhibitors: the first, ADO-like, and the second, a novel alkynylpyrimidine series. The two classes of structures, which contain structurally similar substituents, reveal distinct binding modes in which the AK structure accommodates the inhibitor classes by a 30° rotation of the small domain relative to the large domain. This change in binding mode stabilizes an open and a closed intermediate structural state and provide structural insight into the transition required for catalysis. This results in a significant rearrangement of both the protein active site and the orientation of the alkynylpyrimidine ligand when compared to the observed orientation of nucleosidic inhibitors or substrates.

Introduction

Extracellular concentrations of the endogenous neuromodulator adenosine (ADO) are increased under conditions of metabolic stress and trauma (e.g., pain, inflammation, tissue damage, ischemia, seizure activity, etc.) and act to limit tissue damage and restore normal function[1] by activating members of the P1 receptor family, A_1, A_{2A}, A_{2B}, and A_3 receptors.[2] Increased extracellular ADO concentrations can result in the inhibition of excitatory amino acid (glutamate) release, suppression of free radical formation, and neutrophil adhesion, depending on the phenotype of the tissue involved.[3] Since ADO has a half-life on the order of seconds in physiological fluids,[4] its extracellular actions are restricted to the tissue and cellular sites where it is released.[5] The effects of extracellular ADO are terminated by its reuptake and phosphorylation by ADO kinase (AK; ATP:adenosine 5′-phosphotranferase, EC 2.7.1.20) and via deamination by adenosine deaminase (ADA).[6] By preventing ADO phosphorylation, AK inhibition increases intracellular ADO concentrations, altering the equilibrium of the bidirectional transport systems responsible for ADO reuptake with the net effect of increasing the local concentration of ADO in the extracellular compartment.[7] AK inhibition is a more effective mechanism for increasing extracellular ADO levels than inhibition of the catabolic enzyme ADA, as shown by the comparative efficacy of AK and ADA inhibitors in reducing seizure and nociceptive activity in vivo.[8,9]

The AK enzyme is a member of the ribokinase enzyme family, whose members have been studied structurally by a number of groups. Most notably, the structures of human AK enzyme in complex with inhibitors have been reported,[10] as well as structures of *Toxoplasma gondii* AK both in the apoenzyme form and in complex with inhibitors.[11,12] In addition, structures of *Escherichia coli* ribokinase have been reported both in the apoenzyme form and in complex with adenosine and ADP.[13,14] All members of the ribokinase-like family are thought to catalyze the phosphorylation of a ribose sugar at the 5′ position.

AK is a two-domain protein, with the large domain being a mixed α/β structure reminiscent of a Rossmann fold[15] and the small domain a five-stranded α/β motif that is formed, topologically, by sequence insertion between strands $\beta1$ and $\beta2$ of the larger domain (Figure 1). The large domain is composed of a nine-stranded, primarily parallel β-sheet arrangement with seven crossover α-helices. The fold is similar to other carbohydrate kinases of known structure, such as the ribokinase from *E. coli*. The active site of the enzyme is located at the interface of the large and small domains and is near the generalized nucleotide binding site contained in Rossmann folds. The cofactor ATP has been shown to bind at an adjacent site, which orients the γ-phosphate group near the 5′-end of the sugar moiety of the adenosine molecule.[10]

Studies of both the apo and inhibited forms of *T. gondii* AK have revealed two significantly different conformations of the AK enzyme.[14] The apo form of the enzyme is found to be in an open conformation relative to either the inhibited or ternary complex form of the protein. The conformational change is achieved by a rotation of about 30° of the small domain relative to the larger domain. The result of the opening is that the active site is exposed to the solvent, which presumably allows for the initial binding of the substrate and the cofactors. Upon binding, a conformational switch is presumably triggered, and the two domains rotate into the closed conformation. In the closed conformation, the catalytically important residues of the enzyme

* To whom correspondence should be addressed: phone 847-247-0945; fax 847-938-2478; e-mail steve.w.muchmore@abbott.com.

† Coordinates for the AK−5IT and AK−**2** complexes have been deposited in the Protein Data Bank under accession numbers 2I6A and 2I6B, respectively.

‡ Structural Biology, Abbott Laboratories.

§ Neuroscience Research, Abbott Laboratories.

10.1021/jm060189a CCC: $33.50
Published on Web 10/14/2006

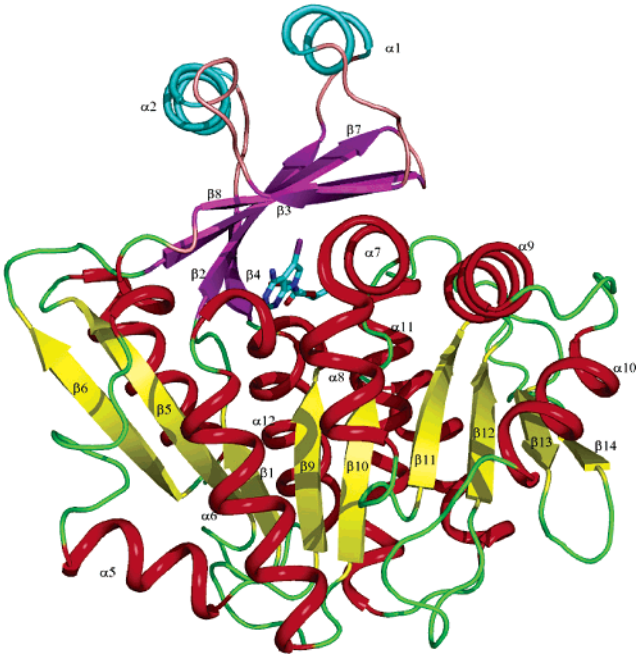

Figure 1. Schematic representation of the structure of human AK bound with a molecule of 5-IT. For the large domain, the α-helices are shown in red and the *β*-strands are shown as directional yellow arrows. The small domain is shown with the helices in cyan and the strands in violet. A stick representation of the 5-IT inhibitor molecule (blue) is shown in the active site, located between the two domains of the protein. The secondary structure elements are labeled consistent with the scheme in Mathews et al.[10]

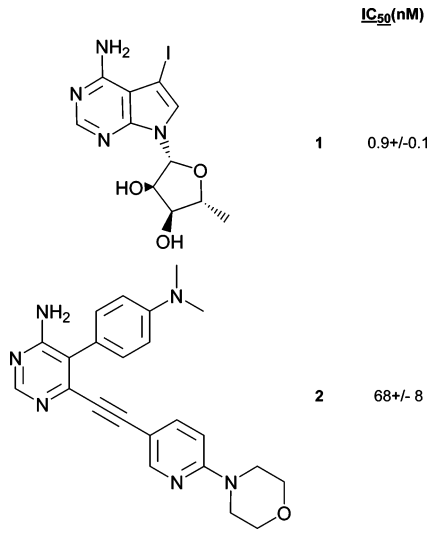

Figure 2. Structures of AK inhibitors and their measured IC_{50} values. Compound **1** is 5-iodo-5′-tubercidin and is an adenosine mimic, while **2** is an example of the alkynylpyrimidine series.

are positioned in close proximity to the cofactor and substrate, and the chemical transformation is achieved.

In this work, we report the crystal structures of human AK in complex with two inhibitors (Figure 2). The first of these is the well-studied AK inhibitor 5-iodotubercidin, **1**, and **2**[16] is a member of a novel alkynylpyrimidine class.[17] As expected, since the molecular structure of 5-iodotubercidin is similar to that of adenosine, the general details of binding interactions of these compounds and the AK protein are similar when the two structures are compared. However, the structure of **2** in complex with human AK is observed to be significantly different from the ADP-containing complexes and is observed to be similar to the apo *T. gondii* structure, in that the inhibitor binds to an open conformation of the protein. Therefore, these two classes of compounds are distinct, in that they exploit two significantly different protein conformations, and constitute one of the few examples of inhibitors of a specific enzyme that have been shown to bind to grossly different conformational states of their target structure.

Experimental Procedures

Protein Cloning and Purification. Human short-form AK was expressed in *E. coli* and purified by use of an adenosine affinity column, the details of which have been published elsewhere.[18] Purified AK was concentrated to 25 mg/mL in a stabilization buffer consisting of 20 mM Tris, pH 7.5, 50 mM potassium chloride, 1 mM sodium azide, 1 mM dithiothreitol, and 10% (v/v) glycerol.

AK Inhibitors. Two potent inhibitors of AK were used in this study, and their structures are shown in Figure 2. The first of these is a well-documented AK inhibitor, 5-iodo-5′-deoxytubercidin[19] (compound **1**). The second, compound **2**, was synthesized in our AK inhibitor program.[16] AK inhibition was measured as previously described.[20] Both compounds produced concentration-dependent inhibition of AK with the following IC_{50} (±SEM, $n = 3$) values: **1**, 0.9 ± 0.1 nM, **2**, 68 ± 8 nM).

Structure Determination. The structure of the AK−5IT protein inhibitor complex was solved by a combination of mid-infrared and density modification techniques. The structure of the AK−**2** complex was solved by molecular replacement with the AK−5IT complex protein structure as the search model. Details of the structure determination and refinement process can be found in the Supporting Information.

Protein Structure Comparisons. Previously reported structures of human and *T. gondii* AK were obtained from the Protein Data Bank and were used unmodified. Single copies of the closed-form human AK structure (PDB code 1BX4) were aligned to the compound **1** structure, while the open form *T. gondii* structure (PDB code 1LIO), was aligned to the structure of compound **2** complex. The coordinates were aligned with the program LSQMAN.[26]

Results

Compound 1 (5-Iodo-5′-deoxytubercidin). Compound **1** is found in a large cavity formed at the interface of the large and small domains (Figure 3A). The iodine atom and the five-member portion of the tubercidin ring of the inhibitor are located in a hydrophobic pocket of the active site, formed by the main-chain atoms of residues 38−40 and 134−136 and the side chains of residues Leu-40, Leu-134, Leu-136, Cys-123, Phe-170, and Phe-201. The iodine atom of the inhibitor is buried deeply into the pocket and is not solvent-accessible. Similar to the previously reported AK−5IT complex structure, the iodine atom of the inhibitor replaces a conserved, highly stabilized water molecule observed in the AK−ADO structure. The exocyclic amine group of the tubercidin ring is found to be in a water-mediated hydrogen-bonding interaction with the main chain of Phe-170 and the side chain of Ser-173. One of the indole nitrogen atoms of the pyrimidine ring interacts with the nitrogen of the side chain of Asn-14, while the other forms a hydrogen-bond interaction with the main-chain nitrogen of the Ser-65 protein residue. The sugar moiety of compound **1** is stabilized by tight interactions of the exocyclic hydroxyl oxygen atoms, forming a salt bridge interaction with the side-chain oxygen atoms of Asp-18. The result of these extensive contacts with the protein is that the protein structure envelopes the inhibitor, sequestering it from the solvent.

Compound 2 [5-(4-(Dimethylamino)phenyl)-6-(6-morpholin-4-ylpyridin-3-ylethynyl)pyrimidin-4-ylamine]. Electron density maps (Supporting Information) showed clear density for the complex and were easily interpreted. The binding mode of **2** is shown in Figure 3B. The compound binds in the same

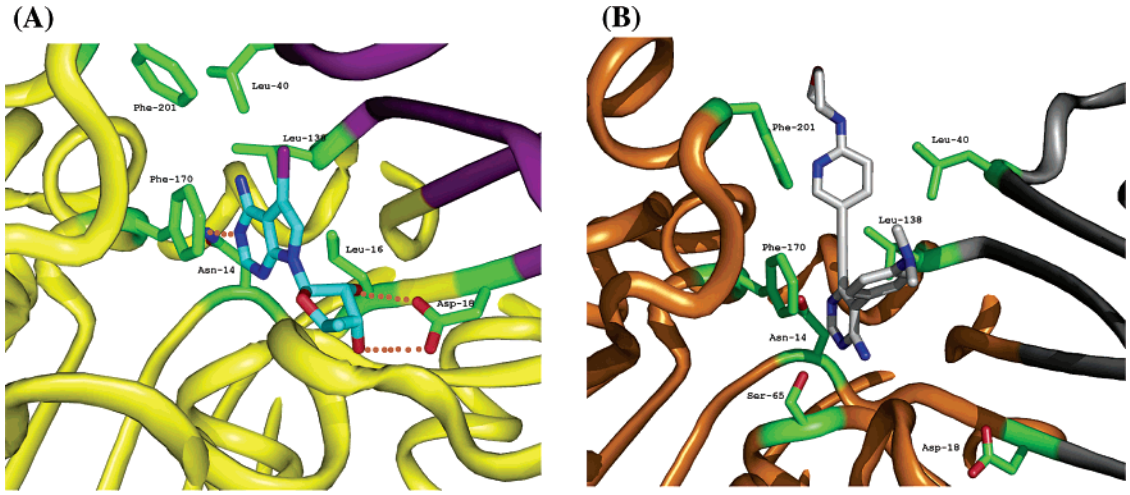

Figure 3. Active-site details for the complexes of human AK and compound **1** (AK−5IT) and **2** (AK−**2**). (A) Active site of the AK−5IT complex. The protein structure of the large domain is shown in yellow ribbon, while the small domain ribbons are colored violet. Side chains of interacting residues, as well as the 5IT inhibitor, are shown in stick representation. (B) Active site of the AK−**2** complex. The point of view is approximately the same as in panel A, and the large domain is colored orange, while the small domain is gray. Note that in the AK−5IT complex, the active site is closed relative to the AK−**2** complex. Most notably, compound **2** disrupts the interaction of Phe-201 with Leu-40. In addition, compound **2** does not interact with Asp-18, which forms a salt-bridge interaction with the sugar moiety in the AK−5IT complex structure.

cleft as ADO and the tubercidin inhibitors. However, the binding of the inhibitor apparently stabilizes an open form of the protein structure (Figure 3B). The interactions of the inhibitor with the protein are significantly different than that of adenosine or **1**. The exocyclic amine of the pyrimidine ring forms a hydrogen-bond interaction with the side-chain hydroxyl of Ser-65, and the only other specific interaction is that of a hydrogen-bond interaction of the ring nitrogen para to the exocyclic amine of the pyrimidine ring. The pyridine ring and portions of the acetylenic linker are sandwiched between the hydrophobic residues Leu-40 and Leu-138 of the small domain and the pair of Phe residues at positions 170 and 201 of the large domain. The morpholine ring is exposed to solvent, and the electron density for the inhibitor at that position is weak, which is reflected by relatively high *B*-factors for the atoms in that ring (data not shown). The specific interactions between the protein and the ribose sugar ring in the AK−5IT complex structure are not observed in the AK−**2** structure.

Protein Structure and Active-Site Comparison. An overlay of the structures of AK inhibited with both **1** and the novel alkynylpyrimidine compound **2** with the large domains aligned is shown in Figure 4. The most striking feature in comparing the two structures is a rigid-body motion of the small domain relative to the large. The extent of this hinge bending motion is measured to be an approximate 30° in the angle between the plane formed by the β-sheet of the large domain and the central β-strands of the small domain. This hinge motion is centered on a Gly-Gly region at residues 68 and 69 and results in a large change in the backbone torsion angles of these residues. This conformational difference is very similar to that observed in the apoenzyme and the AK−ADO−ATP ternary complex of AK from *T. gondii* (Figure 5). However in contrast with the *T. gondii* structures, there is no associated helix-to-coil transition in residues 295−297. This is probably due to the absence of a molecule of ATP in the AK−**2** complex, which is thought to stabilize the formation of an anion hole through interactions with the phosphate atoms of ATP.

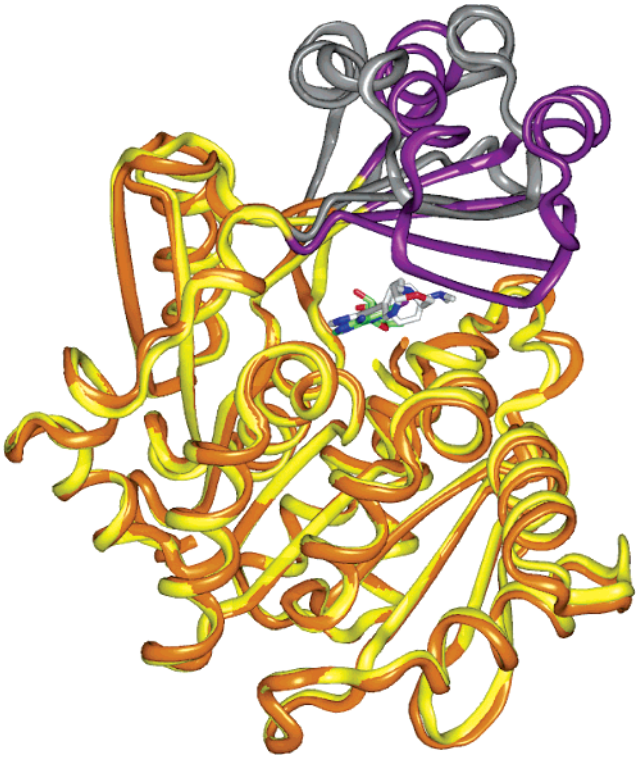

Figure 4. Superposition of the AK−5IT and AK−**2** complex structures. The protein structures have been aligned by use of the coordinates of only the large domain. The small domain of AK is shown to be in two different conformations, related by a rigid-body rotation of approximately 30°. Each of the two domains maintains a similar overall conformation in both of the structures; the largest conformational changes are localized to the hinge region at the proximal end of the β-sheet central to the small domain.

Discussion

Conformational rearrangement upon binding of a ligand or natural substrate is not an unusual observation in protein structural studies.[27] Examples where important, small-scale changes of protein structure upon binding, including the side-chain rearrangement, are well documented and include the active-site rearrangements, movement of side chains of hemoglobin upon O_2 binding,[28] and motion of surface residues. Another form of conformational change, that of the change of the structure of a flexible loop of the protein structure during substrate binding and catalysis, has long been appreciated. A

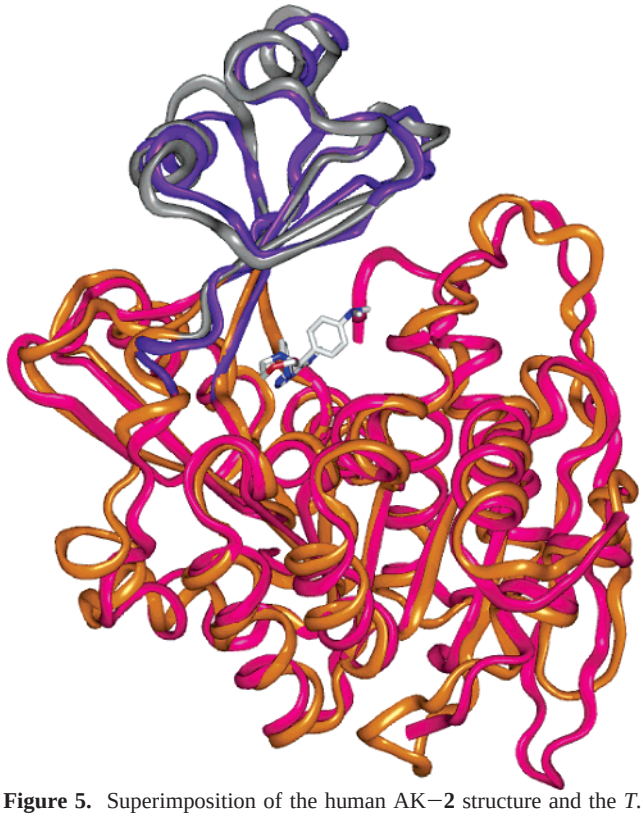

Figure 5. Superimposition of the human AK−**2** structure and the *T. gondii* AK−ADO−AMP-PCP structure. The human AK structure is in orange and gray ribbons, while the *T. gondii* structure is shown in magenta and violet. A model of compound **2** is shown in the active site of the two molecules for reference. In both structures, the enzyme is in an open conformation relative to the conformation observed when adenosine is bound.

classical example of this type of conformational change is observed, for example, in the glycotransferases,[29] in which a small hinged loop rearranges to close the active site during catalytic turnover. The other well-characterized example of conformational change during ligand binding is that of the tyrosine kinases,[30] where two lobes of the protein structure are presumed to move relative to one another to close the active site when the substrates bind.

However, the implications of protein conformational change for structure-based drug design are significant. Small-scale rearrangements of the target protein active site, as observed in the three-dimensional structure, have allowed for the development of new chemical series that take advantage of a rearrangement of the active-site residues.[31] The alkynylpyrimidine series, represented by compound **2**, was thought to bind to AK in a manner analogous to adenosine or the adenosine-like inhibitors in both the ligand and protein conformation. Given the chemical similarity of the pyrimidine ring system in **2** to that of the purine ring system in adenosine (Figure 6), this seemed a reasonable starting point for modeling exercises and provided a rationale for plotting a course for probing the activity of this chemical series. In addition, it had been assumed that the pyrimidine−morpholine moiety was a surrogate of the ribosyl sugar ring (Figure 6a). Modeling studies of compound **2** into the closed form of the AK active site showed that if the similar ring systems superimposed, the morpholine moiety of the inhibitor would be predicted to be in a close-contact clash with protein, in particular, portions of the small domain. The experimental structure of the AK−**2** complex, and the attendant structural rearrangement of the active site (Figure 6b), helps explain the SAR observed for the series. Obviously, when the alkynylpyrimidine compounds were modeled after the adenosine-like inhibitors, a confusing SAR pattern emerged. For example,

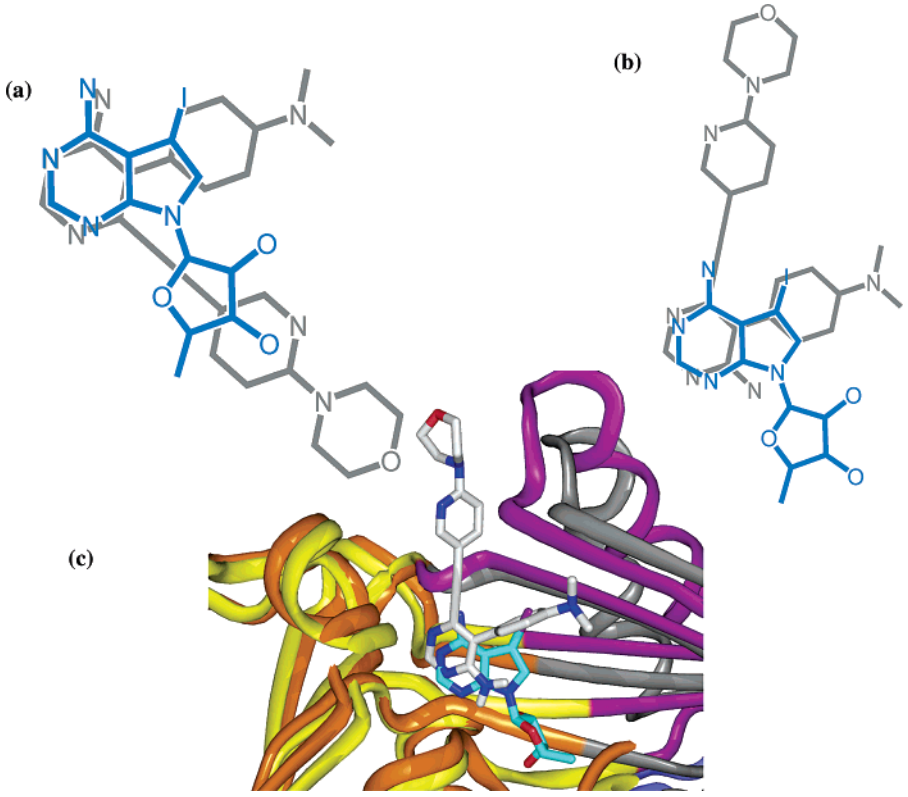

Figure 6. Comparison of the binding modes of compounds **1** and **2**. The assumed (a) and actual (b) overlays of **1** (5IT) (blue) and **2** (gray) show the two-dimensional relationship of the two compounds. (c) Three-dimensional overlay of the crystal structures of AK−5IT and AK−**2** complexes. The structure of the protein for the AK−5IT complex is shown in ribbon representation, with the large domain in orange and the small domain colored gray. For the AK−**2** complex, the large domain is represented in orange ribbon, and the small domain in violet. The inhibitors are shown in stick representation, 5IT in cyan and **2** in gray.

Table 1. General Structure−Activity Relationship of Acetylinic AK Inhibitors

Compound	Structure	AK inhibition (IC_{50})[a]	Compound	Structure	AK inhibition (IC_{50})[a]
3	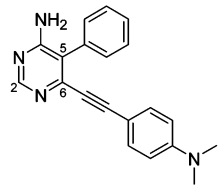	20	**6**	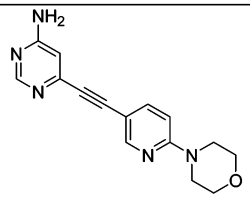	120
4	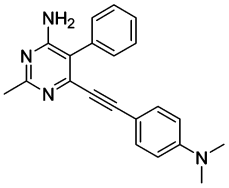	>1000	**7**	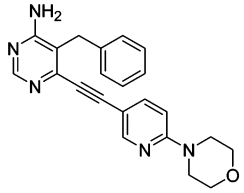	40
5	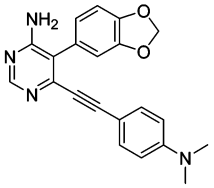	9	**8**	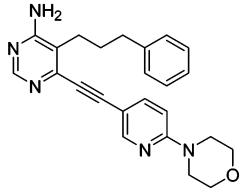	2.5

[a] Assay with cytosolic AK. Mean values for inhibitors (IC_{50}, nanomolar) were calculated from at least three determinations [standard error of the mean (SEM) ≤ 10].

substitutions on the morpholine ring, which would be expected to decrease binding affinity, had little or no effect. If one assumes adenosine-like binding modes for the compounds listed in Table 1, it is difficult to reconcile the SAR with structural models. For example, when compounds **3** and **4** are compared, a significant loss of potency is observed by the addition of a methyl group at position 2 on the pyrimidine ring.[17] This can be explained, in either binding mode, by an anticipated steric clash, particularly with the β-carbon of the side chain of residue Asn-14, which would lead to the disruption of the hydrogen-bonding pattern of the inhibitor series. However, substitutions at the 5 position become more problematic to model with the adenosine structure as a guide. For example, in compound **5**,[17] the substitution of the phenyl group for a benzodioxole group results in a 2-fold gain in potency, even though the molecular models of this compound based on the adenosine binding mode predict significant clashes with the main chain and side chains of residues 38−40 of the small domain and with the side chain of residue Phe-201 of the large domain. Assuming the same orientation of compound **5** to that of compound **2**, the addition of the benzodioxole group would potentially allow for a favorable hydrogen-bond formation, possible involving the side chain of residues Asn-296 and Gln-38.

Another example of difficult to interpret SAR that can be explained by the two binding modes is the series represented by compounds **6**, **7**, and **8**.[16] These compounds show a potency gain with increasing length of linker between the pyrimidine ring and the phenyl group. This gain of potency is not consistent with the adenosine-binding mode, an observation similar to compound **5.** The extension of the linker is not expected to lead to the gain in potency, unless the structure is consistent with the binding mode observed for compound **2.** The most potent compound in this series is **8**, with a measured IC_{50} of 2.5 nM, which is presumably due to the three-carbon flexible linker allowing the phenyl ring to adopt an optimal interaction with the AK protein between the small and large domains. Interestingly, extending the linker to four carbons (structure not shown) leads to a 10-fold loss in potency. This loss of potency could potentially be due to a steric clash with the protein generated by the addition of the longer-chain linker.

Protein rearrangements and ligand binding rearrangements of this type confound efforts to transfer information from one chemical series to another in a drug development project, since in the absence of crystal structure information it is reasonable to assume that overlay of points of molecular similarity can be used to transfer SAR information from one chemical series to another. While this approach is reasonable in most cases, this work illustrates an example where two apparently similar chemical series bind to the target molecule in very different fashions than would be predicted by simply overlaying the inhibitor structures. The difficulty in predicting protein structure rearrangements,[32] particularly of the magnitude described here, underscores the value of structure-based design in guiding drug development efforts.

Acknowledgment. Use of the IMCA-CAT beamline 17-ID at the Advanced Photon Source was supported by the companies of the Industrial Macromolecular Crystallography Association through a contract with the Center for Advanced Radiation Sources at the University of Chicago.

Supporting Information Available: Procedure for structure determination and tables showing data collection, phasing statistics, and refinement statistics. This material is available free of charge via the Internet at http://pubs.acs.org.

References

(1) Williams, M.; Jarvis, M. F. Purinergic and pyrimidinergic receptors as potential drug targets. *Biochem. Pharmacol.* **2000**, *59* (10), 1173−1185.
(2) Ralevic, V.; Burnstock, G. Receptors for purines and pyrimidines. *Pharmacol. Rev.* **1998**, *50* (3), 413−492.
(3) Bong, G. W.; Rosengren, S.; Firestein, G. S. Spinal cord adenosine receptor stimulation in rats inhibits peripheral neutrophil accumulation. The role of *N*-methyl-D-aspartate receptors. *J. Clin. Invest.* **1996**, *98* (12), 2779−2785.

(4) Moser, G. H.; Schrader, J.; Deussen, A. Turnover of adenosine in plasma of human and dog blood. *Am. J. Physiol.* **1989**, *256* (4, Pt 1), C799−C806.
(5) Engler, R. L. Adenosine. The signal of life? *Circulation* **1991**, *84* (2), 951−954.
(6) Arch, J. R.; Newsholme, E. A. Activities and some properties of 5′-nucleotidase, adenosine kinase and adenosine deaminase in tissues from vertebrates and invertebrates in relation to the control of the concentration and the physiological role of adenosine. *Biochem. J.* **1978**, *174* (3), 965−977.
(7) Golembiowska, K.; White, T. D.; Sawynok, J. Modulation of adenosine release from rat spinal cord by adenosine deaminase and adenosine kinase inhibitors. *Brain Res.* **1995**, *699* (2), 315−320.
(8) Zhang, G.; Franklin, P. H.; Murray, T. F. Manipulation of endogenous adenosine in the rat prepiriform cortex modulates seizure susceptibility. *J. Pharmacol. Exp. Ther.* **1993**, *264* (3), 1415−1424.
(9) Kiel, G.; DeLander, G. E. Spinally mediated antinociception is induced in mice by an adenosine kinase, but not an adenosine deaminase inhibitor. *Life Sci.* **1992**, *51*, 171−176.
(10) Mathews, I. I.; Erion, M. D.; Ealick, S. E. Structure of human adenosine kinase at 1.5 A resolution. *Biochemistry* **1998**, *37* (45), 15607−15620.
(11) Cook, W. J.; DeLucas, L. J.; Chattopadhyay, D. Crystal structure of adenosine kinase from *Toxoplasma gondii* at 1.8 A resolution. *Protein Sci.* **2000**, *9* (4), 704−712.
(12) Schumacher, M. A.; Scott, D. M.; Mathews, I. I.; Ealick, S. E.; Roos, D. S.; Ullman, B.; Brennan, R. G. Crystal structures of *Toxoplasma gondii* adenosine kinase reveal a novel catalytic mechanism and prodrug binding. *J. Mol. Biol.* **2000**, *296* (2), 549−567.
(13) Sigrell, J. A.; Cameron, A. D.; Jones, T. A.; Mowbray, S. L. Structure of *Escherichia coli* ribokinase in complex with ribose and dinucleotide determined to 1.8 A resolution: insights into a new family of kinase structures. *Structure* **1998**, *6* (2), 183−193.
(14) Sigrell, J. A.; Cameron, A. D.; Mowbray, S. L. Induced fit on sugar binding activates ribokinase. *J. Mol. Biol.* **1999**, *290* (5), 1009−1018.
(15) Rossmann, M. G.; Argos, P. The taxonomy of binding sites in proteins. *Mol. Cell Biochem.* **1978**, *21* (3), 161−182.
(16) Matulenko, M. A. Manuscript in preparation.
(17) Gomtsyan, A.; Didomenico, S.; Lee, C. H.; Matulenko, M. A.; Kim, K.; Kowaluk, E. A.; Wismer, C. T.; Mikusa, J.; Yu, H.; Kohlhaas, K.; Jarvis, M. F.; Bhagwat, S. S. Design, synthesis, and structure−activity relationship of 6-alkynylpyrimidines as potent adenosine kinase inhibitors. *J. Med. Chem.* **2002**, *45* (17), 3639−3648.
(18) McNally, T.; Helfrich, R. J.; Cowart, M.; Dorwin, S. A.; Meuth, J. L.; Idler, K. B.; Klute, K. A.; Simmer, R. L.; Kowaluk, E. A.; Halbert, D. N. Cloning and expression of the adenosine kinase gene from rat and human tissues. *Biochem. Biophys. Res. Commun.* **1997**, *231* (3), 645−650.
(19) Davies, L. P.; Jamieson, D. D.; Baird-Lambert, J. A.; Kazlauskas, R. Halogenated pyrrolopyrimidine analogues of adenosine from marine organisms: pharmacological activities and potent inhibition of adenosine kinase. *Biochem. Pharmacol.* **1984**, *33* (3), 347−355.
(20) Jarvis, M. F.; Yu, H.; Kohlhaas, K.; Alexander, K.; Lee, C. H.; Jiang, M.; Bhagwat, S. S.; Williams, M.; Kowaluk, E. A. ABT-702 (4-amino-5-(3-bromophenyl)-7-(6-morpholinopyridin-3-yl)pyrido[2,3-*d*]pyrimidine), a novel orally effective adenosine kinase inhibitor with analgesic and antiinflammatory properties: I. In vitro characterization and acute antinociceptive effects in the mouse. *J. Pharmacol. Exp. Ther.* **2000**, *295* (3), 1156−1164.
(21) Otwinowski, Z.; Minor, W. Processing of X-ray Diffraction Data Collected in Oscillation Mode. *Methods Enzymol.* **1997**, *276*, 321−334
(22) CCP4. The CCP4 suite: programs for protein crystallography. *Acta Crystallogr. D: Biol. Crystallogr.* **1994**, *50* (5), 760−763.
(23) Tong, L.; Rossmann, M. G. Rotation function calculations with GLRF program. *Methods Enzymol.* **1997**, *276*, 594−611.
(24) Accelrys. *Quanta Molecular Graphics Program*, San Diego, CA.
(25) Roversi, P.; Blanc, E.; Vonrhein, C.; Evans, G.; Bricogne, G. Modelling prior distributions of atoms for macromolecular refinement and completion. *Acta Crystallogr. D: Biol. Crystallogr.* **2000**, *56* (10), 1316−1323.
(26) Kleywegt, G. J.; Jones, T. A. Software for handling macromolecular envelopes. *Acta Crystallogr. D: Biol. Crystallogr.* **1999**, *55* (4), 941−944.
(27) Gutteridge, A.; Thornton, J. Conformational changes observed in enzyme crystal structures upon substrate binding. *J. Mol. Biol.* **2005**, *346* (1), 21−28.
(28) Perutz, M. F.; Muirhead, H.; Mazzarella, L.; Crowther, R. A.; Greer, J.; Kilmartin, J. V. Identification of residues responsible for the alkaline Bohr effect in haemoglobin. *Nature* **1969**, *222* (200), 1240−1243.
(29) Qasba, P. K.; Ramakrishnan, B.; Boeggeman, E. Substrate-induced conformational changes in glycosyltransferases. *Trends Biochem. Sci.* **2005**, *30* (1), 53−62.
(30) McInnes, C.; Fischer, P. M. Strategies for the design of potent and selective kinase inhibitors. *Curr. Pharm. Des.* **2005**, *11* (14), 1845−1863.
(31) Maring, C. J.; Stoll, V. S.; Zhao, C.; Sun, M.; Krueger, A. C.; Stewart, K. D.; Madigan, D. L.; Kati, W. M.; Xu, Y.; Carrick, R. J.; Montgomery, D. A.; Kempf-Grote, A.; Marsh, K. C.; Molla, A.; Steffy, K. R.; Sham, H. L.; Laver, W. G.; Gu, Y. G.; Kempf, D. J.; Kohlbrenner, W. E. Structure-based characterization and optimization of novel hydrophobic binding interactions in a series of pyrrolidine influenza neuraminidase inhibitors. *J. Med. Chem.* **2005**, *48* (12), 3980−3990.
(32) Elber, R. Long-timescale simulation methods. *Curr. Opin. Struct. Biol.* **2005**, *15* (2), 151−156.

JM060189A